hanced mixing between the ligand p and metal d orbitals with increasing polarizability of X.[6a] The band structures of NbI_4 calculated in the present work are consistent with this view. The width of the valence band and the band gap are respectively ~0.3 and ~0.8 eV in NbI_4, while the corresponding values are respectively ~0.1 and ~1.0 eV in $NbCl_4$. Figure 11 shows that the lone-pair orbital n of the terminal ligands lies far below the d-block orbital in $NbCl_4$ but slightly above the $d_{x^2-y^2}^+$ orbital in NbI_4. The proximity of the n and $d_{x^2-y^2}^+$ levels in NbI_4 causes the valence band to have mixed-orbital characters, largely n near the zone center but $d_{x^2-y^2}^+$ near the zone edge.

Concluding Remarks

The halide-bridged $[PtL_4{\cdot}PtL_4X_2]^{4+}$ and NbX_4 chains share a common structural feature; i.e., each chain has two metal-bridging halide bonds of unequal lengths alternating along the chain direction. We found this structural feature well reproduced by the total energies per unit cell calculated from their one-electron band structures. The singly bridged $[PtL_4{\cdot}PtL_4X_2]^{4+}$ chain provides a partially filled band when all the metal-bridging halide bonds become identical in length while the doubly bridged NbX_4 chain, like the triply bridged VS_3^{2-} chain reported elsewhere,[8c] leads to partially filled overlapping bands even if the lengths of the two alternating metal-bridging halide bonds are not exactly the same. However it is noted that a Peierls distortion[2,3] such as the pairing 7 → 6 of the doubly bridged NbX_4 chain does not occur in $BaVS_3$ which consists of the triply bridged VS_3^{2-} chains.[13]

Acknowledgment. This work was supported by the donors of the Petroleum Research Fund, administered by the American Chemical Society. M.-H. Whangbo is grateful to Triangles Universities Computer Center for generous computer time.

Registry No. $[Pt(NH_3)_4{\cdot}Pt(NH_3)_4Cl_2]^{4+}$, 75400-13-4; $[Pt(NH_3)_4{\cdot}Pt(NH_3)_4Br_2]^{4+}$, 75400-14-5; NbI_4, 13870-21-8; $NbCl_4$, 13569-70-5.

(13) (a) Takano, M.; Kosugi, H.; Nakamura, N.; Shimada, M.; Wada, T.; Koizumi, M. *J. Phys. Soc. Jpn.* **1977**, *43*, 1101. (b) Massenet, O.; Ruder, R.; Since, J. J.; Schlenker, C.; Mercier, J.; Kelber, J.; Stucky, G. D. *Mater. Res. Bull.* **1978**, *13*, 187.
(14) Ammeter, J. H.; Bürgi, H.-B.; Thibeault, J. C.; Hoffmann, R. *J. Am. Chem. Soc.* **1978**, *100*, 3686.
(15) Clementi, E.; Roetti, C. "Atomic and Nuclear Data Tables"; Academic Press: New York, 1974; Vol. 14, p 177.
(16) Hinze, J.; Jaffe, H. H. *J. Phys. Chem.* **1963**, *67*, 1501.

Contribution from the Research Laboratories, Eastman Kodak Company, Rochester, New York 14650

Electronic Properties of Metal Clusters: Size Effects

R. C. BAETZOLD

Received April 21, 1980

The effects of size are examined from some properties of model metal clusters by using molecular orbital calculations. Electronic effects were examined for a variety of clusters up to 79 atoms for Au, Ru, Rh, and Pd. In this size range, the binding energy and density of states change drastically with size. We find that p orbitals play a role in the bonding of these clusters, which increases with size. The charge distribution in these clusters results in excess surface electrons as a result of narrower surface bands. Adsorption energies of H_2, C_2, or O_2 molecules on different clusters show a widely varying size dependence, which can be related to electronic properties of the cluster. The addition of ligands to a hypothetical cluster $Rh_6(CO)_x$ (x = 2, 6, 12, 16) changes the metal atom DOS to reflect properties of a smaller bare metal cluster.

Introduction

Metal clusters, naked or coordinatively saturated, have been studied from many viewpoints. Experimental approaches to the study of clusters include synthetic,[1] catalytic,[1] chemisorptive,[2] and spectroscopic[3-5] methods. Inherent in many of these studies is the cluster–surface analogy. This analogy deals with the electronic and chemisorptive properties of small metal clusters and their ability to adequately represent metal surfaces. Much of the experimental and theoretical evidence dealing with this question has been discussed.[1,2] A detailed correlation of electronic and chemisorptive properties of small clusters with cluster size would be helpful in probing this analogy.

The synthesis of many cluster compounds[6] of various compositions such as the $Rh_n(CO)_m$ (n = 2-14) series makes possible the systematic study of metal properties. Naked metal clusters have been formed by decarbonylation of these cluster compounds under suitable conditions[7] or by evaporation under vacuum.[8] Hamilton and co-workers have reported catalytic data involving nickel electroless-deposition reactions on naked metal clusters prepared by evaporation,[8] showing effects of cluster size. In each of these studies, the role of ligands in influencing catalytic properties and the extent to which cluster electronic properties represent the analogous surface properties are unknown.

In this paper we examine some electronic properties of clusters as a function of cluster size and as a function of the presence of ligands. In approaching this problem, we use relatively simple molecular orbital calculations such as the extended Hückel theory,[9] which yield valuable insight into the modes of bonding and qualitative trends in behavior of these systems. This method is quite versatile and similar to the tight-binding method useful in solid-state physics. We rely heavily upon experimental information which has been reported for the spectroscopic properties of metal clusters. More

(1) Muetterties, E. L.; Rhodin, T. N.; Band, E; Brucker, C. F.; Pretzer, W. R. *Chem. Rev.* **1979**, *79*, 91.
(2) Moskovits, M. *Acc. Chem. Res.* **1979**, *12*, 229.
(3) Ozin, G. A.; Huber, H.; McIntosh, D. *Inorg. Chem.* **1977**, *16*, 3078.
(4) Unwin, R.; Bradshaw, A. M. *Chem. Phys. Lett.* **1978**, *58*, 58.
(5) Mason, M. G.; Gerenser, L. J.; Lee, S.-T. *Phys. Rev. Lett.* **1977**, *39*, 288. Mason, M. G.; Hamilton, J. F.; Lee, S.-T.; Nellis, B. F.; Gerenser, L. J.; Logel, P. C., unpublished work.
(6) Longoni, P.; Chini, P. *J. Am. Chem. Soc.* **1976**, *98*, 7225.
(7) Smith, G. C.; Chojnacki, T. C.; Dasgupta, S. R.; Iwatate, K.; Watters, K. L. *Inorg. Chem.* **1975**, *14*, 1419.
(8) Hamilton, J. F.; Logel, P. C. *Photogr. Sci. Eng.* **1974**, *18*, 507; *J. Catal.* **1973**, *29*, 253.
(9) Hoffmann, R. *J. Chem. Phys.* **1963**, *39*, 1397.

0020-1669/81/1320-0118$01.00/0

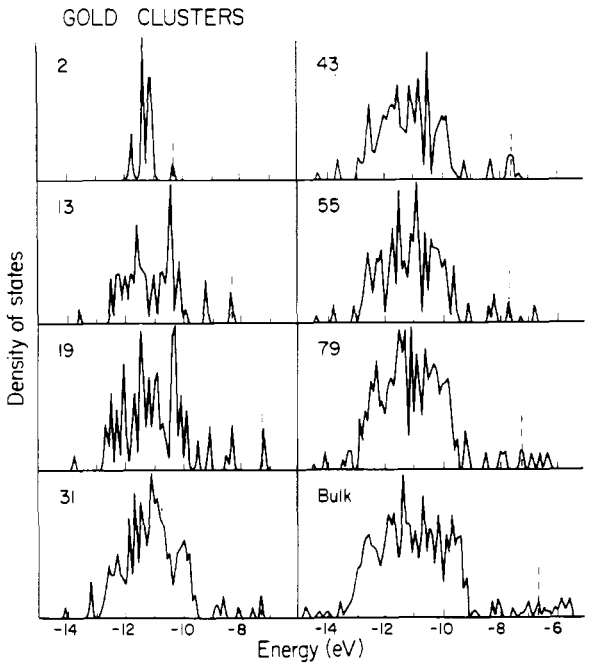

Figure 1. Density-of-states plots for fcc spherical gold clusters resulting from summing 0.1 eV fwhm Gaussian functions for each energy level. The dotted line denotes the HOMO level for each sized cluster. The dominant peaks are due to d orbitals with some s, p hybridization.

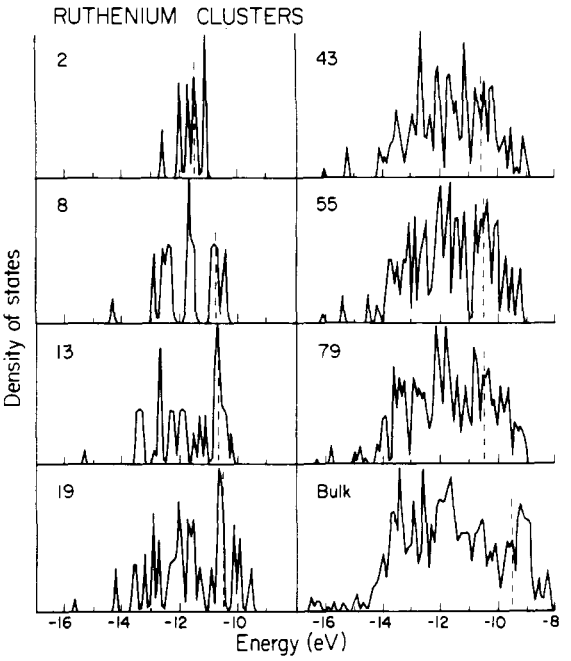

Figure 2. Density-of-states plots for fcc spherical ruthenium clusters resulting from summing 0.1 eV fwhm Gaussian functions for each energy level. The dotted line denotes the HOMO level for each sized cluster.

sophisticated ab initio calculations have also been applied such as the work of Schaefer et al.[10] on Be_n clusters and by Goddard et al.[11] on Ni_n clusters. Various approximations, however, are required to apply such complicated methods to complex cluster systems, and it is useful to compare results from a number of diverse calculational procedures.

In this study we examine the effects of size on clusters of some metal atoms. Our prior studies[12] were extended to 79-atom clusters, where comparison was made with the bulk-calculated density of states (DOS). In addition to examining cluster electronic properties, we compare chemisorptive properties for some simple molecules.

Small clusters, even in the size range of 79 atoms, contain many surface atoms. Spherical clusters with the face-centered-cubic (fcc) geometry and complete shells were considered when we examined 13-, 19-, 43-, 55-, and 79-atom clusters. The average coordination number for this series increases as 4.6, 6.3, 7.3, 7.8, and 8.1, respectively. Thus, even the 79-atom cluster has only two-thirds of the bulk coordination, which is 12 in the fcc structure. It should be expected that many properties of the 79-atom cluster will deviate significantly from the bulk. We also examined some fcc clusters with sizes intermediate between the clusters with full shells of nearest neighbors.

Results

A. Electronic Properties. The DOS behavior of bare metal clusters offers a means of monitoring the convergence of cluster electronic properties toward the bulk properties. Let us consider this property for gold. The bonding in gold clusters is determined largely by the 6s and 6p valence orbitals. The average calculated electronic configuration changes from $s^{1.04}p^{0.03}d^{9.93}$ at Au_2 to $s^{0.90}p^{0.11}d^{9.99}$ at Au_{13} to $s^{0.90}p^{0.29}d^{9.81}$ at Au_{43}, which indicates the increasing component of p bonding in larger clusters. The s and p orbitals are much more diffuse than the d orbitals, and they form a broad band which completely overlaps the d band at a cluster size of 13 atoms. Figure 1 shows the DOS calculated for gold clusters and indicates the rather slow approach to bulk behavior with increasing cluster size. The most intense portion of these spectra is due to d orbitals. Significant gaps in the d portion of the DOS persist up to 31-atom sizes, where they begin to fill in, but certain portions of energy space remain unoccupied even at 79 atoms. The 79-atom cluster has a bulklike DOS, although agreement in every detail would require an even larger cluster.

It is interesting to compare the DOS curves of Ru with those of Au clusters. Gold has a filled atomic d shell which remains essentially d^{10} in the cluster, whereas atomic Ru is d^8, and this configuration changes with size for the cluster and the bulk. In Ru clusters the bonding is due to s and d orbitals, with some lesser amounts due to p orbitals. The d orbitals contribute a strong measure of bonding energy in Ru because of their partial occupation, which does not require occupation of all the antibonding orbitals.

The DOS for Ru clusters is shown in Figure 2 as a function of cluster size. The Fermi energy falls within the d band, which contains closely packed molecular orbitals, and there is a high density of vacant d orbitals at this position. The small Ru clusters contain d molecular orbitals with significant spacings between one another. These spacings are quite apparent even up to the 79-atom cluster. The gaps result from crystal field interaction and require additional delocalizing interaction to fill in. This behavior is most apparent in Ru, as opposed to other metal clusters, because of the wide d band. We observe s molecular orbitals completely overlapping the d band in Ru, beginning at the 8-atom size. The broadening of this band to ~−16.5 eV can be seen in the DOS curves for different sizes, and it is clear that the effect occurs throughout this size range. The behavior observed for Au and Ru as a function of particle size is also observed for Pd, Rh, and Ag clusters.

It should be emphasized that the convergence to bulk behavior in Figures 1 and 2 is not parameter dependent. We used identical parameters and approximations for the bulk and

(10) Dykstra, C. E.; Schaefer, H. F.; Meyer, W. *J. Chem. Phys.* **1976**, *65*, 5141. Schaefer, H. F. *Acc. Chem. Res.* **1977**, *10*, 287.
(11) Melius, C. F.; Upton, T. H.; Goddard, W. A., III. *Solid State Commun.* **1978**, *28*, 501.
(12) Baetzold, R. C. *J. Chem. Phys.* **1978**, *68*, 555; **1971**, *55*, 4363. Baetzold, R. C. *J. Phys. Chem.* **1978**, *82*, 738.

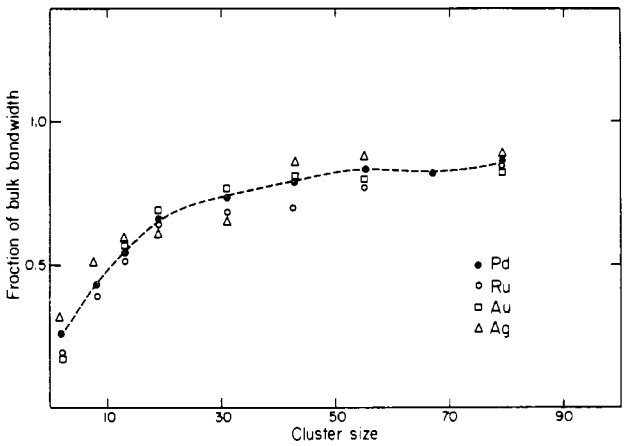

Figure 3. Fraction of bulk d bandwidth calculated for Ru, Pd, Ag, and Au clusters plotted vs. size of the fcc cluster.

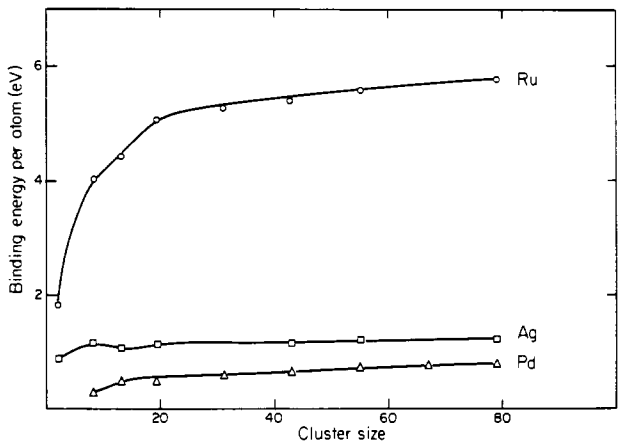

Figure 4. Binding energy per atom calculated for Ru, Ag, and Pd clusters plotted vs. size of the fcc cluster.

cluster calculations so that any size dependence on parameters is removed in determining the degree of convergence to the bulk. A comparison of absolute values such as bandwidths is parameter dependent, but no attempt has been made to fit these calculated results to any experiment or other calculation. Nevertheless, the d bandwidths calculated for bulk metals are realistic compared to other solid-state-physics calculations (Ag, 2.7 eV and 3.4 eV;[13] Rh, 4.5 eV and 5.5 eV[14]). Although the bulk calculated DOS curves could be modified by suitable parameter choice to agree better with some other calculated result such as the APW or RAPW methods commonly used in solid-state physics, this is not attempted here. We only emphasize that qualitatively the bulk calculated DOS agrees with that calculated by other methods.

The bandwidth of the metal clusters increases with increasing cluster size and can be used as a guide to the convergence to bulk. The curve in Figure 3 shows the d bandwidth (greatest separation of predominant d levels) for several different metal clusters plotted as percentage of the bulk value vs. cluster size. Each metal cluster has a curve of the same shape, and the bandwidth is proportional to the square root of the average coordination number. This relation is expected from model considerations within the tight-binding method.[15] In addition to the broadening of d bands (Figure 3), the s band spreads at a similar rate. Although the largest clusters considered have a d bandwidth of 0.86 of the bulk value, we estimate the value 0.91 of the bulk at an average coordination number of 9 and 0.96 of the bulk at an average coordination number of 10, which indicates that very large clusters are required for properties to converge to the bulk limit. These data compare favorably with experimental measurements of DOS. Unwin and Bradshaw[4] used ultraviolet photoemission spectroscopy to measure DOS of palladium clusters on carbon. They found that d-level emission broadens as a function of increasing particle size and estimate 140 atoms for bulk convergence. Mason et al.[5] used ESCA to investigate several transition-metal clusters adsorbed on carbon or silicon dioxide and found that 100–200 atoms are required for "bulklike" spectra.

The binding energy is quite different for the various types of metal atom clusters. Figure 4 shows a plot of behavior vs. size for Ru, Ag, and Pd clusters. Ruthenium clusters have a rapidly increasing binding energy per atom which asymptotically approaches some upper limit. The binding energies are much greater than for Ag or Pd, partly because the d band of Ru is incompletely filled. The average electronic configuration at Ru_{43} is $s^{0.72}p^{0.32}d^{6.96}$, which indicates the significant role that the valence s and p orbitals have in bonding. The small Ru clusters have similar configurations: Ru_2, $s^{0.96}p^{0.05}d^{6.99}$; Ru_8, $s^{0.71}p^{0.16}d^{7.13}$; Ru_{13}, $s^{0.68}p^{0.22}d^{7.10}$. In palladium the d band is not fully occupied, but the binding energy is much less than for Ru. The binding energy per atom increases fairly linearly with size (Figure 4). The configuration found for large Pd clusters is noted in Table I. In gold clusters, all binding comes from s, p orbital interactions, since the d shell remains essentially full. The binding energy (Figure 4) is rather flat.

Table I. Properties of Large Metal Clusters[a]

property	Ag_{79}	Au_{79}	Pd_{79}	Ru_{79}	Rh_{79}
% of bulk d bandwidth	89	82	86	85	87
diff between measd ionizn potential and bulk calcd value, eV	0.34	0.54	0.29	0.85	0.30
gap between HOMO and LUMO, eV	0.11	0.09	0.01	0.08	0.01

[a] Calculated configuration for M_{43}: Ag, $s^{0.83}p^{0.30}d^{9.87}$; Au, $s^{0.90}p^{0.29}d^{9.81}$; Pd, $s^{0.52}p^{0.04}d^{9.44}$; Ru, $s^{0.72}p^{0.32}d^{6.96}$; Rh, $s^{0.30}p^{0.20}d^{8.50}$.

Table II. HOMO Value (eV) Calculated for Metal Clusters

size	Ag	Au	Ru	Pd
2	8.60	10.28	11.06	10.58
13	7.07	8.13	10.65	10.31
19	6.63	7.43	10.52	10.11
31	6.67	7.29	10.66	9.96
43	6.63	7.60	10.63	9.89
55	6.75	7.68	10.54	9.95
79	6.51	7.28	10.55	9.89
bulk	6.17	6.70	9.70	9.60

The gap between highest occupied molecular orbital (HOMO) and lowest unoccupied molecular orbital (LUMO) is a measure of metallic properties. The spacing kT is expected and at room temperature is ~0.02 eV. The HOMO and LUMO of silver clusters give a representative measure of this effect. A significant gap between these levels decreases with size; the gap is 0.1 eV at 79 atoms for Au and Ag but not for Rh, Pd, and Ru, because the HOMO and LUMO fall in the d band. When the requirement that a metal have spacing of kT between energy levels is invoked, those s-conduction-band metals like Ag and Au require much larger cluster sizes than Rh, Ru, and Pd for bulk behavior.

A considerable decrease in HOMO takes place with increasing cluster size, as expected. The development of a band structure with occupied antibonding levels is partly responsible for the decrease in ionization potential on progressing from

(13) Christensen, N. E. *Phys. Status Solidi B* **1972**, *54*, 551. Barrie, A.; Christensen, N. E. *Phys. Rev. B* **1976**, *14*, 2242.
(14) Christensen, N. E. *Phys. Status Solidi B* **1973**, *55*, 117.
(15) Haydock, R.; Kelly, M. J. *Surf. Sci.* **1973**, *38*, 139.

Table III. Average Charges of M_{43} Cluster

metal	1 atom shell 1 (inside)	12 atoms shell 2	6 atoms shell 3	24 atoms shell 4 (outside)
Ag	−0.076	+0.090	−0.050	−0.030
Au	+0.072	+0.190	+0.002	−0.10
Ru	+0.92	+0.99	+0.02	−0.54
Pd	+1.00	+0.68	−0.21	−0.33

atom to bulk. This effect with size is shown in Table II for several clusters. The larger shifts calculated for Ag and Au occur because the HOMO falls in the s, p band, which is much broader than the d band. In those clusters where the d occupation changes considerably with size (such as Pd and Ru), we need to include the effect of orbital occupancy in computing the overall shift in ionization potential. For example, increasing the d occupation of Pd from d^9s to d^{10} results in a decrease of 3.17 eV in the d orbital energy.[16] Thus, for a final state of $d^{9.44}$, about half of the 3.17 eV would be required in addition to the orbital destabilization to account for the decrease in ionization potential.

The comparison of electronic cluster properties with bulk properties shows several differences. Table I shows that none of the 79-atom clusters has a d bandwidth greater than 89% of the bulk. The ionization potential decreases with cluster size, but for all of the 79-atom clusters, it is a few tenths of an electronvolt greater than the bulk value. Likewise, the gap between HOMO and LUMO is greater than kT (0.02 eV at room temperature) for 79-atom clusters of Ag, Au, and Ru, but not for Pd or Rh. This suggests that conduction properties of Pd_{79} or Rh_{79} may be bulklike, but this is not true for the other metals. Although these properties approach the bulk property, the 79-atom cluster is not bulklike in many respects. However, the general shape of the DOS is close to bulklike.

The charge distribution, which is calculated with a Mulliken-type analysis, places a negative charge on the surface of these clusters. The largest clusters for which charges were calculated have 43 atoms and four shells of atoms. Table III lists the average charge for atoms within each shell for various clusters with use of non-self-consistent EH approach. Clearly, the charge separation is too large to be consistent with potential considerations for Ru and Pd, but it is much more realistic for Ag and Au. Small adjustments in the potential could cause large charge readjustments in clusters with partly filled d bands. Nevertheless, the negative charge is predicted on the cluster surface, because the projection of the DOS for a surface atom is narrower than this projection for a bulk atom. This follows from considering the average number of nearest neighbors, which is the factor leading to the interactions which broaden bands. Hence, in a nearly filled band, more charge will be located in atoms which have a narrower projected DOS. We emphasize that self-consistent calculations would act to reduce the charge separation but not the direction of charge excess. It should also be expected from this consideration that, for metals with bands less than about half full, the charge distribution will be reversed.

B. Chemisorption Effect. The binding energy for a series of molecules adsorbed to Au, Rh, and Ru clusters has been calculated as a function of cluster size. A correlation of these trends with changes in electronic properties would be useful in correlating electronic with chemisorptive properties. Adsorbate molecules, including H_2, O_2, and C_2, were placed between two metal atoms of the cluster in a di-σ site (i.e., adsorbate bond parallel to metal bond). The adsorbate–metal distance was determined by the sum of covalent radii. This adsorption site was maintained for all cluster sizes. Although other possible sites may be the preferred binding site in some situations, maintaining a constant site allowed us to test the influence of electronic properties on chemisorptive properties.

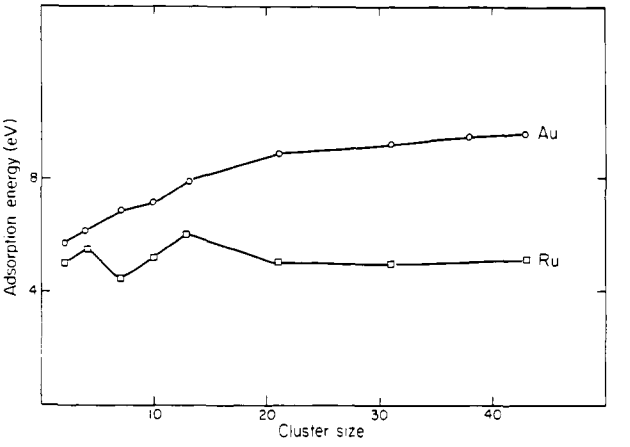

Figure 5. Absorption energy of C_2 to Ru and Au clusters at a constant di-σ site plotted *vs.* cluster size. The cluster geometry is fcc.

The binding energy of the C_2 adsorbate to Ru clusters is shown in Figure 5. Although there are some irregularities at the smaller clusters, the binding energy becomes constant at a small cluster size. A similar size dependence is found for H_2 and O_2.[17] When this behavior is compared with the DOS behavior (Figure 2), we conclude that electronic and chemisorptive properties do not scale the same way with cluster size. We find a similar behavior for the same adsorbate molecules on Rh clusters.

The binding energy to gold clusters shows a strong dependence on particle size. Figure 5 shows considerable changes in the C_2 binding energy up to the 43-atom size. This trend in binding energy is similar for O_2 and H_2[17] and scales with trends in DOS (Figure 1) or HOMO (Table II). Although the binding energy varies strongly with Au cluster size, charge transferred and certain energy levels are insensitive to cluster size. For example, the charge per H atom is −0.10 for each Au cluster size, and the σ_g level which contains predominant orbitals of H_2 is −17.83 for adsorption to Au_2, −17.84 for Au_4, and −17.88 for Au_{21}, Au_{31}, and Au_{43}.

The greater sensitivity of adsorbate binding energy to cluster size of Au compared to Ru emphasizes the variety of effects which may be found. Clearly a local-bonding model is more appropriate for Ru than Au. This may be due to the composition of orbitals near the HOMO, which are more delocalized s, p orbitals in the case of Au rather than the more localized d orbitals in the case of Ru. Changes of binding energy with size are due to small mixing of orbitals from the adsorbate with many different cluster orbitals. Thus, the greater sensitivity of orbital energy (HOMO) to size for Au may lead to this size effect. A complete analysis of these interactions is required and may explain experimentally reported size effects in heterogeneous catalysis.[18]

C. Ligand Effect. Some hypothetical complexes of rhodium were examined to determine how ligands modify the electronic properties of the metal cluster framework. Let us consider $Rh_6(CO)_{16}$, where the metal atoms are arranged as an octahedron with 12 CO ligands bonded terminally and four in triangular bridge positions.[19] We consider the computed DOS for the full molecule and then remove CO ligands, starting first with the bridge positions. There are many similar complexes which could be considered.[20]

(16) Determined by averaging the electronic energies of the multiplet states.

(17) Baetzold, R. C., unpublished data available upon request.

(18) Boudart, M. In "Advances in Catalysis"; Eley, D., Pines, H., Weisz, P., Eds.; Academic Press: New York, 1969; p 153.

(19) Corey, E.; Dahl, L.; Beck, W. *J. Am. Chem. Soc.* **1963**, *85*, 1202.

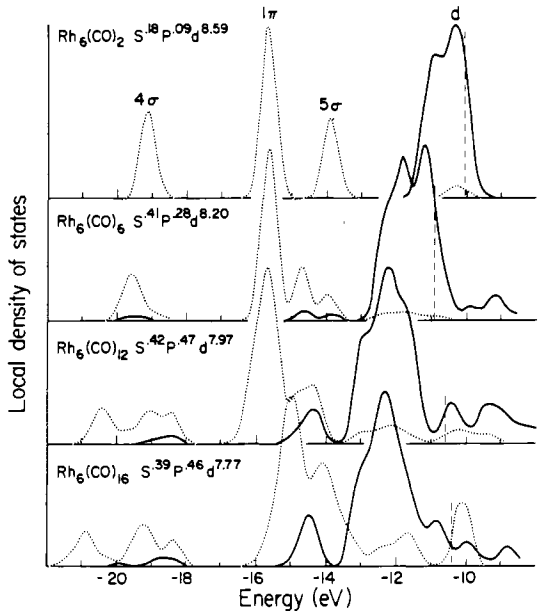

Figure 6. Density of states for the metal component (solid) and ligand component (dotted) in $Rh_6(CO)_x$ clusters (x = 2, 6, 12, 16). Gaussian functions of 0.5 eV fwhm were summed for each energy level to obtain the normalized curve. The dashed line near −10 eV denotes the highest occupied molecular orbital (HOMO). The orbital character of the dominant CO orbitals is indicated as well as the average Rh population.

The local DOS in $Rh_6(CO)_{16}$ shows a dependence of electronic properties upon composition. This effect is illustrated in Figure 6. The Rh density is indicated by solid lines and the CO density by dotted lines. Note that the DOS at the Fermi energy (HOMO) is strongly modified by the number of CO ligands attached to the Rh framework. At low substitution, the metal component is very large at the Fermi energy, but at higher CO substitution the Fermi energy occurs in a region of much lower metal atom density. This occurs because the Rh atom d orbitals are destabilized by mixing with the CO molecular orbitals and are shifted closer to the vacuum.

There is a net electron withdrawal from the Rh cluster, giving an average Rh charge of +0.38 on $Rh_6(CO)_{16}$. This effect is accompanied by a reduction of d occupation with increasing CO substitution, as shown in Figure 6. This reduction in d occupation caused by ligands is opposite to the increase in d occupation of bare clusters which accompanies increasing cluster size.[12] The ligands have significantly reduced cluster metallic properties by decreasing the d occupation and $D(E_F)$.

The ultraviolet photoemission spectra have been reported[21] for $Rh_6(CO)_{16}$ and CO on Rh(III) surfaces.[22] We would like to qualitatively compare the DOS calculated for the CO component with these experimental spectra. In $Rh_6(CO)_{16}$ or chemisorbed CO on Rh(III), only two peaks due to CO orbitals are reported in the region up to 15 eV below the Fermi energy. The low-binding-energy peak is thought to be composed of the 1π and 5σ orbitals of CO, and the other peak is assigned as 4σ. These assignments are the results of an extensive set of calculations[23] and experiments[24] treating CO chemisorbed on nickel and other transition-metal systems. This spectrum contrasts to the gas-phase[25] CO spectrum, where three distinct peaks are observed with the 5σ level positioned 2 eV closer to vacuum than 1π and 4σ at 3 eV lower than 1π. We may compare these results with our computations in Figure 6. Clearly the 5σ and 1π levels shift together as the degree of CO substitution increases. The appearance of density due to CO orbitals takes place throughout the Rh d band region. These orbitals located near the Fermi energy are $2\pi^*$ molecular orbitals which are becoming populated. These effects are consistent with experimental measurements on these systems and point to decreasing metallic character with CO ligand substitution.

Table IV. Parameters of the Calculation

atom	orbital	$-H_{ii}$, eV	exponent	d orbital coeff
Ru	5s	10.14	2.078	
	5p	6.13	2.078	
	4d	11.52	5.378	0.5573
			2.303	0.6642
Rh	5s	9.30	2.135	
	5p	5.97	2.135	
	4d	12.18	5.542	0.5823
			2.398	0.6405
Pd	5s	7.57	1.568	
	5p	1.84	1.568	
	4d	10.99	5.983	0.5264
			2.613	0.6372
Ag	5s	7.56	2.244	
	5p	3.83	2.244	
	4d	11.58	6.070	0.5889
			2.663	0.6370
Au	6s	9.22	2.602	
	6p	4.37	2.602	
	5d	11.09	6.163	0.6851
			2.794	0.5696

Conclusions

We have used extended Hückel procedures to show that some properties of bare metal clusters up to 79 atoms in size are different from bulk properties. These include DOS, IP, level spacing, and orbital occupation. The changes in these electronic properties correlate well with photoemission data. In addition, the electronic properties can be related to chemisorptive properties of the bare cluster. The degree of delocalization of the upper part of the occupied valence orbitals appears to play an important role in determining size effects in the cluster.

Addition of ligands to a bare cluster offers a means of altering electronic properties. In the case of CO ligands added to Rh_6 we find changes in the cluster DOS, orbital occupation, and $D(E_F)$ which are generally associated with smaller bare clusters. In addition, the metal cluster is depleted of electrons, which should make it a good electron acceptor.

Acknowledgment. I am grateful to Evgeny Shustorovich for helpful conversations on this work.

Appendix

All calculations were performed by using the extended Hückel procedure.[9] An iterative charge- and configuration-dependent procedure was employed for Ru, Rh, and Pd clusters up to 19 atoms in size. Noniterative procedures were employed for the larger clusters and also for all clusters of Ag and Au. Spherical fcc geometries only were considered. For the noniterative calculations, data for the Hamiltonian elements were obtained from the values at convergence of the central atom in M_{19}. Parameters used for the Hamiltonian elements were obtained from Hartree–Fock wave functions[26] and atomic

(20) Martinengo, S.; Heaton, B. T.; Goodfellow, R. J.; Chini, P. *J. Chem. Soc., Chem. Commun.* **1977**, 39.
(21) Conrad, H.; Ertl, G.; Knozinger, H.; Kuppers, J.; Latta, E. E. *Chem. Phys. Lett.* **1976**, *42*, 115.
(22) Brann, W.; Neumann, M.; Iwan, M.; Koch, E. E. *Phys. Status Solidi B* **1978**, *90*, 525.
(23) Blyholder, G. *J. Phys. Chem.* **1974**, *68*, 2772.
(24) Allyn, C. L.; Gustafsson, T.; Plummer, E. W. *Chem. Phys. Lett.* **1977**, *47*, 127. Broden, G.; Rhodin, T. N.; Brucker, C.; Benbow, R.; Hurych, Z. *Surf. Sci.* **1976**, *59*, 593.
(25) Turner, D. W.; Baker, C.; Baker, A. D.; Brundle, C. R. "Molecular Photoelectron Spectroscopy"; Wiley: New York, 1970.
(26) Basch, H.; Gray, H. B. *Theor. Chim. Acta* **1966**, *4*, 367.

spectra,[27] and final converged values are listed in Table IV. Double-ζ Slater orbitals were used to represent the d orbitals, and single-ζ Slater orbitals were used for s and p orbitals.

No attempt was made to fit our calculated results to other results or experimental data. The secular equation was solved by using the standard Wolfsberg-Helmholz[28] formula for off-diagonal terms (eq 1). The parameters used for cluster

$$H_{ij} = \tfrac{1}{2}KS_{ij}(H_{ii} + H_{jj}) \qquad K = 1.75 \qquad (1)$$

calculations were then employed for bulk calculations through the use of Bloch functions, by using procedures described in earlier work.[12] The bond length in all clusters and the bulk was 2.5 Å.

The density-of-states curves were calculated by using Gaussian functions of 0.1 eV fwhm. These functions were centered on each energy level and summed. The normalized sums were then plotted as the density of states. Binding energies were calculated as energy differences between cluster and all of the isolated atoms by using eq 2, where E = energy,

$$E = \sum_i E_i N_i \qquad (2)$$

E_i = energy of molecular orbital i, and N_i = occupation, as in standard calculations.[9] A Mulliken-type analysis[29] was used to determine the orbital populations.

Registry No. Ag, 7440-22-4; Au, 7440-57-5; Pd, 7440-05-3; Ru, 7440-18-8; Rh, 7440-16-6; $Rh_6(CO)_{16}$, 28407-51-4.

(27) Moore, C. E. *Natl. Bur. Stand. (U.S.) Circ.* **1949**, *No. 467*, Vol. 1-3.
(28) Wolfsberg, M.; Helmholz, L. *J. Chem. Phys.* **1953**, *20*, 837.
(29) Mulliken, R. S. *J. Chem. Phys.* **1955**, *23*, 1833.

Contribution from the School of Chemical Sciences, University of Illinois, Urbana, Illinois 61801

Spin-Crossover Ferric Complexes: Curiosities Observed for Unperturbed Solids

MUIN S. HADDAD,[1] MICHAEL W. LYNCH, WAYNE D. FEDERER,[2] and DAVID N. HENDRICKSON*

Received July 14, 1980

The preparation and characterization of a series of spin-crossover ferric complexes with the composition $[Fe(X\text{-}SalEen)_2]Y$, where X-SalEen results from the Schiff-base condensation of X-substituted salicylaldehyde and *N*-ethylethylenediamine, are reported. Several of the complexes exhibit a gradual, but complete, spin-crossover transition from high spin to low spin in the solid state, whereas certain complexes exhibit an incomplete transition and there is a "plateau" in the μ_{eff}/Fe vs. temperature curve. One compound, $[Fe(3\text{-}OCH_3\text{-}SalEen)_2]PF_6$, experiences a sudden spin-crossover phase transition. The conversion from high spin to low spin occurs within a 2° range around the temperature 159 K. A sensitivity of physical properties to exact compound preparation is demonstrated. In spite of the variation in the series, it is shown by variable-temperature ^{57}Fe Mössbauer and EPR techniques that only two electronic states, the high-spin $^6A_1$ excited state and one low-spin Kramers doublet ground state, are thermally populated for any of the compounds. There is no evidence of an intermediate-spin state. The ground-state Kramers doublet in these complexes has one unpaired electron in an orbital which is largely d_{xy} in composition.

Introduction

Several iron(II) and iron(III) complexes exhibit properties characteristic of "spin-equilibrium" complexes, where a high-spin excited state is within thermal energy of the low-spin ground state.[3] Many studies have focused on determining the types of ligands that lead to a "spin-equilibrium" complex and whether ligand substituents affect the equilibrium. Only very recently has there been significant progress in answering a fundamental yet more difficult question, namely: What are the kinetics and mechanisms of spin state interconversions? Spin transitions are believed to play an important role in biological systems, and spin equilibria in certain hemoproteins may be coupled to electron transport.[4] For spin-crossover iron complexes in solution, magnetic susceptibility data yield approximately linear log K vs. $1/T$ plots, consistent with a dynamic equilibrium between the two spin states where K is the equilibrium constant. In fact, relaxation techniques have been used to measure "spin-flipping" rates for complexes in solution.[5-7]

"Spin-equilibrium" compounds in the solid state seldom give linear plots of log K vs. $1/T$. Several curiosities have been observed for spin-crossover iron(II) and iron(III) complexes in the solid state. First, the variation of the effective magnetic moment (μ_{eff}) per iron ion (or molar paramagnetic susceptibility) vs. temperature for a given complex does not correspond simply to a Boltzmann distribution over the thermally populated high-spin and low-spin states. For the ferric dithiocarbamate spin-crossover complexes, for example, *apparently* successful theoretical fits of the susceptibility data could only be obtained by assuming a temperature-dependent energy separation between the high-spin and low-spin states together with a temperature-dependent vibrational partition coefficient.[8] Infrared data, however, do not support such assumptions.[8,9] Almost discontinuous (i.e., occurring over a few degrees) high-spin to low-spin transitions have been noted for a number of iron(II) complexes,[10] which could also be a manifestation of something more than a simple Boltzmann distribution.

A second curiosity observed in the solid state for spin-crossover complexes is an incompleteness of the transition at

(1) University of Illinois Fellow, 1976-1979.
(2) 3M Fellowship, 1979-1980.
(3) For the most recent reviews, see: (a) Goodwin, H. A. *Coord. Chem. Rev.* **1976**, *18*, 293. (b) Martin, R. H.; White, A. H. *Transition Met. Chem.* **1968**, *4*, 113.
(4) Dose, E. V.; Tweedle, M. F.; Wilson, L. J.; Sutin, N. *J. Am. Chem. Soc.* **1977**, *99*, 3887.
(5) Dose, E. V.; Hoselton, M. A.; Sutin, N.; Tweedle, M. F.; Wilson, L. J. *J. Am. Chem. Soc.* **1978**, *100*, 1141.
(6) Beattie, J. K.; Binstead, R. A.; West, R. J. *J. Am. Chem. Soc.* **1978**, *100*, 3044.
(7) Binstead, R. A.; Beattie, J. K.; Dose, E. V.; Tweedle, M. F.; Wilson, L. J. *J. Am. Chem. Soc.* **1978**, *100*, 5609.
(8) Hall, G. R.; Hendrickson, D. N. *Inorg. Chem.* **1976**, *15*, 607.
(9) Sorai, M. *J. Inorg. Nucl. Chem.* **1978**, *40*, 1031.
(10) König, E.; Ritter, G.; Irler, W.; Nelson, S. M. *Inorg. Chim. Acta* **1979**, *37*, 169 and references therein.

0020-1669/81/1320-0123$01.00/0